



**University of
Zurich**^{UZH}

**Zurich Open Repository and
Archive**

University of Zurich
University Library
Strickhofstrasse 39
CH-8057 Zurich
www.zora.uzh.ch

Year: 2018

An industrial design solution for integrating NMR magnetic field sensors into an MRI scanner

Kennedy, Michael ; Lee, Yoo Jin ; Nagy, Zoltan

Abstract: Purpose: Neuroimaging research relies on the skills of increasingly multidisciplinary individuals and often requires the installation and use of additional home-built or third-party equipment. The purpose of the present work was the safe, ergonomic, durable, and aesthetically pleasing installation of magnetic field monitoring equipment into a scanner, while keeping the setup compatible with standard operating procedures. Methods: An extensive set of steps was required to design a 3D printed solution to install a magnetic field camera into the eight-channel head coil of a 3T MRI scanner. First, the outer surface of the plastic coil housing was recreated into a 3D model, and the installation of the magnetic field sensors around this 3D model was performed in a virtual environment. The 3D printed solution was then assembled and tested for safety, reproducible performance, and image quality. Results: The 3D printed solution holds the probes in stable positions and guides the necessary cables in an organized fashion and away from the volunteer. Assembly is easy and the solution is ergonomic, durable, and safe. We did not find excessive heating in the 3D printed parts, nor in the electronics, that they help to incorporate. The material used interferes minimally with transmit math formula field. Conclusion: he design met all of the boundary conditions for a durable, safe, cost-effective, attractive, and functional installation. This work will provide the basis for installing the magnetic field sensors into other available head coils, and for designing the experimental setup for projects with varying experimental requirements. Magn Reson Med, 2017. © 2017 International Society for Magnetic Resonance in Medicine.

DOI: <https://doi.org/10.1002/mrm.27055>

Posted at the Zurich Open Repository and Archive, University of Zurich

ZORA URL: <https://doi.org/10.5167/uzh-146570>

Journal Article

Accepted Version

Originally published at:

Kennedy, Michael; Lee, Yoo Jin; Nagy, Zoltan (2018). An industrial design solution for integrating NMR magnetic field sensors into an MRI scanner. Magnetic Resonance in Medicine, 80(2):833-839.

DOI: <https://doi.org/10.1002/mrm.27055>

An Industrial Design Solution for Integrating NMR Magnetic Field Sensors into a Magnetic Resonance Imaging Scanner

Michael Kennedy^{1,2}, Yoojin Lee^{1,3} and Zoltan Nagy^{1,3}

¹ Laboratory for Social and Neural Systems Research, University of Zurich, Switzerland

² Department of Design, Industrial Design Unit, Zurich University of the Arts, Switzerland

³ Institute of Biomedical Engineering, ETH, Zurich, Switzerland

Running title: Incorporating Magnetic Field Sensors into a MRI Scanner

Word count: 2800

Correspondence to	Zoltan Nagy
	Laboratory for Social and Neural Systems Research
	University Hospital Zurich
	Rämistrasse 100
	P.O. Box 149
	Zürich
	Switzerland

Key words: industrial design, MRI, magnetic field monitoring, dynamic field camera 3D printing, biomedical engineering, multidisciplinary, 3T

ABSTRACT

Purpose:

Neuroimaging research relies on the skills of increasingly multidisciplinary individuals and often requires the installation and use of additional home-built or 3rd party equipment. The purpose of the present work was the safe, ergonomic, durable and aesthetically pleasing installation of magnetic field monitoring equipment into a scanner while keeping the set up compatible with standard operating procedures.

Methods:

An extensive set of steps was required to design a 3D printed solution to install a magnetic field camera into the 8-channel head coil of our Philips 3T MRI scanner. First, the outer surface of the plastic coil housing was recreated into a 3D model and the installation of the magnetic field sensors around this 3D model was performed in a virtual environment. The 3D printed solution was then assembled and tested for safety, reproducible performance and image quality.

Results:

The 3D printed solution holds the probes in stable positions and guides the necessary cables in an organized fashion and away from the volunteer. Assembly is easy and the solution is ergonomic, durable and safe. We did not find excessive heating in the 3D printed parts nor in the electronics that they help to incorporate. The material used interferes minimally with transmit B_1^+ field.

Conclusions:

The design met all the boundary conditions for a durable, safe, cost effective, attractive and functional installation. This work will provide the basis for installing the magnetic field sensors into other available head coils and to design experimental set up for projects with varying experimental requirements.

Key words: industrial design, MRI, magnetic field monitoring, dynamic field camera, 3D printing, biomedical engineering, multidisciplinary, 3T

INTRODUCTION

Many research fields are becoming increasingly multidisciplinary. For example in imaging neuroscience, successful completion of a project may require skills in MRI theory, statistics, neuroanatomy, computer programming as well as psychology, medicine or biology. In addition, experiments often require the fusion of technologies and equipment, be it third-party or home-built, and an integration into a specialized environment. This could be MRI compatible tactile stimulators (e.g. Fig. 1 in (1)), devices monitoring volunteer behavior (e.g. Fig. 1 in (2)) or robotic systems (e.g. Fig. 4 in (3)) – to mention but a few. Installation of such equipment in a safe, ergonomic and durable manner that is also easy on the eye put constraints on both design and manufacturing. Often equipment must serve a large group of end-users, many of whom will not be experts in the specialized technology. Hence, to achieve a final product that is compatible with the specialized environment, easy to handle, meets ethical guidelines, lasts long, and is aesthetically pleasing will demand additional skills that fall well outside the above-mentioned and already wide array of expertise.

In our case the task was the installation of a clip-on magnetic field camera (Skopec Magnetic Resonance Technologies AG, Zurich, Switzerland) into a standard 3T MRI scanner for neuroimaging research.

Magnetic field monitoring (4,5) enables independent measurement of spatio-temporal magnetic field dynamics during the operation of an MRI scanner. The additional information collected can be incorporated into the image reconstruction pipeline to alleviate or eliminate image artifacts. For example, fast imaging methods that are often used in functional (6) and diffusion MRI (7) can be corrected for ghosts, blurring, physiological artifacts and eddy current distortions (8-11).

The installation of this equipment into an MRI scanner required forethought and multidisciplinary expertise, including industrial design and manufacturing processes. Achieving a safe, ergonomic, durable and cost effective installation that was also compatible with established procedures of functional and structural neuroimaging experiments was nontrivial. The aim of this paper was to describe the design and installation procedure and list the required steps in enough detail that a reader could achieve a similar installation. Our 3D-printable design will be publicly available to serve as a current best practice for those who intend to make an identical installation or use this design as a starting point for their specific requirements.

METHODS

Design

A clip-on magnetic field camera performs an NMR experiment on small drops of a doped Fluorine compound (12,13). The entire system consists of several components, not all of which are relevant for this paper. The actual magnetic field sensors (14) that need to be installed near the imaging volume of interest will be the focus of this report and henceforth referred to as *probes*, while the housing of the active front-end electronics as *Tx/Rx box*.

The installation of the clip-on magnetic field camera was made for a 3T Philips Achieva MRI scanner (Philips Healthcare, Best, The Netherlands). The probes themselves were installed within the 8-channel SENSE head coil (henceforth *8ch coil*). The original design of this widely-used coil was made by Invivo (Gainseville, FL, USA) and sold through various scanner manufacturers.

Our solution required a 3D model of the plastic housing of the 8ch head coil. Because such a 3D model was not available from the vendor, we resorted to CT scanning the coil and using freely available software packages 3D Slicer (15), Meshlab (16), Meshmixer (<http://www.meshmixer.com>) as well as the proprietary Solidworks suite (<http://www.solidworks.com>) to recreate it. The CT scans were acquired with a Siemens Somatom Force CT (Siemens Healthcare, Erlangen Germany) scanner at 600.0 μm isotropic resolution and a 512 x 512 acquisition matrix.

To reconstruct the computer aided design (CAD) model in Solidworks the image slices of the CT scan were used as a reference. These images were aligned with and scaled to measurements of the cross sectional diameter of the coil in the mid sagittal slice and then solid parametric surfaces were drawn manually to match the outer surface of the plastic housing of coil. While this model parametric offered the usual benefits of parametric CAD models its correspondence to the actual physical coil was not perfect. Therefore, a separate 3D model was created using 3D slicer, Meshlab and Meshmixer, against which the CAD model could be checked. The reason for this second 3D model and the steps required for its creation are detailed in the supplemental material.

Supporting Table S1 lists boundary conditions for the installation of the probes into the 8ch head coil. The flow chart in Fig. 1 provides details toward the final design.

Insert Figure 1 about here

Arranging the probes around the imaging volume of interest is at the discretion of the user but the constellation of the 16 probes is not entirely arbitrary. For a given SNR of the raw probe signals, the error propagated into the estimation of k-space trajectory measurement is a function of the x, y, z coordinates of the 16 probes (see Eq. 8 in (4)). Additionally, fMRI experiments require a line of sight to visual stimuli. Therefore, an iterative procedure was required until an arrangement was found that did not hinder fMRI scanning but was well conditioned for spherical harmonic fitting to the probe data.

Care was also taken that the homogeneity of the B_0 field was minimally disturbed near the probes. The 3D printing material (nylon powder, *PA 2200 supplied by Electro Optical Systems*) was tested prior to manufacturing. To minimize influence on the MRI data quality, an ultra-short TE sequence helped ascertain it was not MR visible. For compatibility with field monitoring its magnetic susceptibility was checked to ensure it was not para-/ferro-magnetic.

3D printing was by www.shapeways.com.

Experiments

Four different experiments were performed. In Experiment 1 we tested the robustness of the set up in terms of reproducibility. Every experiment with the magnetic field camera requires a calibration of the spatial position of the probes. On different days of 4 consecutive weeks the probe positions were calibrated 10 times in a row. This was followed by three iterations of a diffusion-weighted MRI scan and two additional calibrations of the probe positions. The diffusion-weighted scan contained one b_0 image and 64 diffusion weighted images with a b-value of 1000 s/mm^2 . The purpose was to shake the scanner couch and hence test the capacity of the probe holder insert to keep the probes in place. The Euclidean distance from the isocentre was measured for each probe in each calibration.

The purpose of Experiment 2 was to ascertain the safe operation of our set up (17). We used an infrared camera (TiS20, Fluke Corporation, Everett, WA, USA) and took images before and after a 10-minute long scan that provided maximum head SAR in three different configurations: (1) the 8ch head coil on its own, (2) the 8ch head coil along with the 3D printed parts and (3) the entire assembly with the 8ch head coil, 3D printed parts as well as the probes, cables and Tx/Rx box. The MRS Loading Sphere (General Electric, Waukesha, WI) was used as an imaging phantom and test load.

In Experiment 3 we collected five consecutive B_1^+ maps with the actual flip angle method (18) for each of the three configurations in Experiment 2. Configuration 1 with the 8ch coil on its own was repeated on a different day to assess test/re-test variability. For each scan we also recorded the RF power calibration from the scanner log files. The recorded variable (*drive_scale*) is related to the necessary reference voltage required for a 90° RF pulse and also to the relative B_1^+ efficiency of the empty body coil.

The purpose of Experiment 4 was to demonstrate that the entire set up could deliver the expected high quality images. A healthy adult male volunteer was scanned in accordance with guidelines of the local ethics committee. A diffusion MRI dataset identical to Experiment 1 was acquired with concurrent magnetic field monitoring. The offline reconstruction combined the MRI and probe data.

RESULTS

Design and installation

Figure 2 illustrates aspects of the final design. The probes were arranged so that none would be in front of either eye. Even though the resulting optimal arrangement of the probes was not left-right symmetric, the insert was designed in such a way that it would provide an identical obstruction of view to both eyes (red arrows). The insert contained no sharp edges near the probes (blue arrows). The platform for the Tx/Rx box was fastened to the base of the coil with screws (Fig. 2D), which ensured minimal cabling length that was constant during the operation of the coil (note: this coil slides horizontally to aid positioning of the volunteer). The original design of the 8ch head coil includes a tray that supports the head of the volunteer. This tray does not have enough clearance from the inside bottom surface of the coil

to accommodate probes positioned underneath it. Our design includes grooves that allow optimal positioning of the probes while avoiding the weight of the head to transfer to the probes (yellow arrows). A durable, safe and ergonomic design had to avoid loose cabling in or around the head coil. The clips on the probe holder insert and the larger ring on the back of the coil (green arrows) ensure such an arrangement.

Insert Figure 2 about here

Many other features were incorporated into the final design, which were answers criteria set out in Supporting Table S1. The probe holder insert was printed with a regular grid of small holes through which small drops of glue could be applied to fix the insert to the head coil semi-permanently. This helped stabilize the probes against subject movement during experiments but still allowed easy dismounting of the probe set up. The surfaces of the 3D printed parts can be easily coated and wiped to maintain hygiene. To aid installation and dismounting of the probes, the insert was printed with three large slits on the bottom that are visible in Fig. 2 A, B and C and Supplemental Video 1. These slits allow the insert to be slightly squeezed and thus ease the placement of the insert into the head coil. The slits also allow sliding of the feet of the head holding tray, while the feet help avoid the weight of the head transferring to the probes.

Installation of the final set up into the scanner environment is depicted in Fig. 3. Supplemental Video 1 provides a more informative account of the design and manufacturing processes and presents the final product as well.

Insert Figure 3 about here

Experiments

The results of Experiment 1 are depicted in Figure 4. The calibration measurements on different days provide highly reproducible results with maximum 40 μm change in the Euclidean distance of any probe from the isocentre.

Thermal imaging in Experiment 2 did not detect any significant temperature elevation on either the phantom or the coil set up. The maximum surface temperature in any of the 3 configurations was 34.4 °C, which is below body temperature and well below the safety limit (17). It is notable that the surface temperature of a powered but idle 8ch coil without any 3D printed parts or probes can be up to 31.9 °C.

Insert Figure 4 about here

In Experiment 3 it was determined that conductive parts in the probes and cabling increases the RF calibration factor (drive_scale) by about 13% (Configuration 3). No such increase in RF power demand could be detected for the case where only the 3D printed parts were in place. In fact in Configuration 2 (i.e. 8ch coil and the 3D printed parts) the drive_scale was 4.3% lower. Repeated experiments on different days with the 8ch coil on its own (Configuration 1) can lead to 3.4% difference in the drive_scale setting, which is similar in magnitude to adding the 3D printed plastic parts into the 8ch head coil. The uniformity of the B_1^+ field in terms of standard deviation over the entire volume was also found to be variable in the repeated acquisitions of Configuration 1 (10.3% and 10.8%). Adding the 3D printed parts did not make a significant change while incorporating both the 3D printed and the electronic parts increased the standard deviation only to 11.2%.

Figure 5 displays images from a diffusion-weighted imaging data set in Experiment 4. Notable are the lack of Nyquist ghosts or eddy current distortions between the b_0 image (left) and the two diffusion-weighted images. These images are single shot, single average and without employing any parallel imaging.

Insert Figure 5 about here

DISCUSSION

We provided a detailed description of the steps involved in installing a clip-on magnetic field camera into a 3T MRI scanner. The final design adhered to a large number of constraints to ensure a safe, ergonomic, durable and attractive installation that was also compatible with the standard operating procedure of the scanner

during cognitive neuroimaging experiments. Aspects of safety and robustness of the set up were also confirmed with specifically designed experiments.

Apart from arriving at an elegant, functional and practical installation, the design procedure presented in this paper also aided manufacturing. Because the model was available before delivery of the system the minimal required cable lengths between the probes and the Tx/Rx box could be calculated *in silico* and provided to the manufacturer for a bespoke installation.

Arriving at a visually pleasing installation was a key boundary condition. We considered this aspect important because cognitive neuroscience laboratories usually involve naïve subjects who may even be involved in clinical drug trials or take part in experiments where apprehension is a confounding factor. Although we do not know of evidence to support this, we hypothesized that an installation that looks like a risky experiment would lead to or increase unwanted sources of variance (e.g. movement, attention drift, deeper and/or more rapid breathing or increased heart rate) in the MRI data.

Although for this particular installation 3D reconstruction of the coil housing from a CT scan of the 8ch coil was a necessary step, the design procedure could have been greatly simplified had a CAD model of the MRI head coil housing been available from the manufacturer. It may also be possible to recreate the coil housing by depth sensing cameras and 3D surface reconstruction methods that use such data. We did not yet test this technology but may investigate it further if CT scanning becomes an impractical option.

Head coils with 32 or more channels are widely available. Apart from the high number of channels, these coils are also made smaller to optimize SNR (e.g. (19)) resulting in a dense arrangement of metallic components under the plastic covering. Because CT scans are susceptible to artifacts from metallic objects, reconstructing a 3D model of the coil housing will be more difficult and requiring additional manual correction. Although, suppressing metal artifacts may be possible (20-22), investigating its merit was beyond the scope of this work.

It was of paramount importance that emergency procedures would not be hindered by the installation. To remove an unresponsive volunteer from the scanner, our original procedure involved leaving the volunteer inside the 8ch head coil and removing the entire table top from the scanner room prior to the arrival of the crash team. Because the probes are attached to the head coil on one end and to the

Faraday cage on the other end, rapidly removing the 8ch head coil from the room is no longer possible. Our new emergency procedure accommodates leaving the head coil in the scanner room but the volunteer has to be removed from it. Therefore, the design for the installation of the probes had to maintain the capacity for the horizontal sliding back of the coil. Hence, loose cabling or fixing the Tx/Rx box permanently to the base of the coil instead of the movable part were unacceptable solutions.

Although, not explicitly illustrated in the flow chart of Fig. 1 the 3D printing procedure was iterated with several details that were refined incrementally. For example, it became clear only after the first assembly that the Tx/Rx box needed to be secured to the platform (see red circle in Fig. 2) more firmly. Otherwise, during operation the weight of the cable to the Faraday cage pulled the Tx/Rx box away from the probes and the 8ch head coil. Similarly, the first 3D printed insert was about 1mm too large, despite all our careful effort to build the 3D model to scale *in silico*.

Fully complying with IEC standards was beyond the capacity of our laboratory. However, we followed the recommendations of Hoffmann et al (17) in designing Experiment 2 and many other reasonable aspects of safety, like avoiding sharp edges, using a biocompatible material etc. It is also important to note that IEC standards require reproducible experiments to be run to establish whether a set up is acceptable. Indeed, the proposed (or similar) solution that holds the cables, probes and electronic parts in consistent positions may in fact be necessary to produce the required data to obtain IEC approval of the entire set up (i.e. including the 8ch head coil, our 3D printed solution and the magnetic field probes).

The 3D printed parts and the changes made to the 8ch head coil to incorporate the magnetic field probes were not CE approved as a whole. However, to the best of our knowledge, the original CE marking of the 8ch coil will remain valid because the changes made to it are reversible. Lack of CE marking for a set up is not unlike most 7T MRI scanners, third-party MRI receive and/or transmit coils or the magnetic field camera itself. The lack of CE marking does not hinder research activities in general but ethical applications must mention this fact. At our center, ethical approval has been granted for a research study involving healthy adults, a 7T scanner, a clip-on magnetic field camera and a Nova Medical transmit-receive coil.

In summary, the installation of 3rd party equipment into the scanner room may require skills that are not usually possessed by members of neuroimaging

laboratories. The large number of boundary conditions that must be met for a safe, ergonomic, cost effective and aesthetic installation present challenges that require industrial design expertise to curtail. Several future and ongoing projects will benefit from the work reported here. For example, installation of the probes into other MRI head coils can be based on the present design albeit with careful considerations of the details because most other coils do not slide back and forth but rather their top is removable. The 3D model of the 8ch head coil, probes and probe holder insert also will be beneficial for two ongoing projects: building a custom made head stabilization system for high-resolution imaging experiments and creating cost effective and highly precise holders for phantoms (Supporting Fig. S1).

ACKNOWLEDGEMENTS

This work was supported by Swiss National Science Foundation grants (nr. 31003A_166118 and nr. 316030_164076). The authors would like to thank Ms. Beate Kolb, Ms. Susan Rätzer and Ms. Anja Tiessen at the Institute for Diagnostic and Interventional Radiology of the University Hospital Zurich and Mr. Karl Treiber at the Laboratory for Social and Neural Systems Research at the University of Zurich, for their friendly and expert assistance with CT scanning. Dr. Christoph Barmet, Dr. David Brunner of Skope Magnetic Resonance Technologies AG and Dr. Bertram Wilm from the Institute of Biomedical Engineering at the ETH in Zurich kindly spared time for fruitful discussion and guidance throughout the execution of this project. Dr. Markus Scheidegger from Philips Healthcare in Switzerland was instrumental in ensuring the installation and this report were compatible with the manufacturer of our scanner and Dr. Roger Luechinger kindly advised on safety standards.

References

1. Huang R-S, Chen C-F, Tran AT, Holstein KL, Sereno MI. Mapping multisensory parietal face and body areas in humans. *Proceedings of the National Academy of Sciences* 2012;109(44):18114-18119.
2. Hidler J, Hodics T, Xu B, Dobkin B, Cohen LG. MR compatible force sensing system for real-time monitoring of wrist moments during fMRI testing. *J Neurosci Methods* 2006;155(2):300-307.
3. Tsekos NV, Khanicheh A, Christoforou E, Mavroidis C. Magnetic resonance-compatible robotic and mechatronics systems for image-guided interventions and rehabilitation: a review study. *Annu Rev Biomed Eng* 2007;9:351-387.
4. Barmet C, De Zanche N, Pruessmann KP. Spatiotemporal magnetic field monitoring for MR. *Magn Reson Med* 2008;60(1):187-197.
5. Dietrich BE, Brunner DO, Wilm BJ, Barmet C, Gross S, Kasper L, Haeberlin M, Schmid T, Vannesjo SJ, Pruessmann KP. A field camera for MR sequence monitoring and system analysis. *Magn Reson Med* 2015;.
6. Kwong KK, Belliveau JW, Chesler DA, et al. Dynamic magnetic resonance imaging of human brain activity during primary sensory stimulation. *Proc Natl Acad Sci U S A* 1992;89(12):5675-5679.
7. Turner R, Le Bihan D, Maier J, Vavrek R, Hedges LK, Pekar J. Echo-planar imaging of intravoxel incoherent motion. *Radiology* 1990;177(2):407-414.
8. Kasper L, Bollmann S, Vannesjo SJ, Gross S, Haeberlin M, Dietrich BE, Pruessmann KP. Monitoring, analysis, and correction of magnetic field fluctuations in echo planar imaging time series. *Magn Reson Med* 2014;74(2):396-409.
9. Vannesjo SJ, Wilm BJ, Duerst Y, Gross S, Brunner DO, Dietrich BE, Schmid T, Barmet C, Pruessmann KP. Retrospective correction of physiological field fluctuations in high-field brain MRI using concurrent field monitoring. *Magn Reson Med* 2015;73(5):1833-1843.
10. Wilm BJ, Nagy Z, Barmet C, et al. Diffusion MRI with concurrent magnetic field monitoring. *Magn Reson Med* 2015;74(4):925-933.
11. Wilm BJ, Barmet C, Gross S, Kasper L, Vannesjo SJ, Haeberlin M, Dietrich BE, Brunner DO, Schmid T, Pruessmann KP. Single-shot spiral imaging enabled by an expanded encoding model: Demonstration in diffusion MRI. *Magn Reson Med* 2017;77(1):83-91.

12. Barmet C, Wilm BJ, Pavan M, Keupp J, Mens G, Pruessmann KP. Concurrent higher-order field monitoring for routine head MRI: an integrated heteronuclear setup. In: Proceedings of the 18th Annual Meeting of ISMRM, Stockholm, Sweden. 2010;216.
13. Wilm BJ, Barmet C, Pavan M, Pruessmann KP. Higher order reconstruction for MRI in the presence of spatiotemporal field perturbations. *Magn Reson Med* 2011;65(6):1690-1701.
14. De Zanche N, Barmet C, Nordmeyer-Massner JA, Pruessmann KP. NMR probes for measuring magnetic fields and field dynamics in MR systems. *Magn Reson Med* 2008;60(1):176-186.
15. Fedorov A, Beichel R, Kalpathy-Cramer J, Finet J, Fillion-Robin J-C, Pujol S, Bauer C, Jennings D, Fennessy F, Sonka M. 3D Slicer as an image computing platform for the Quantitative Imaging Network. *Magnetic resonance imaging* 2012;30(9):1323-1341.
16. Cignoni P, Callieri M, Corsini M, Dellepiane M, Ganovelli F, Ranzuglia G. Meshlab: an open-source mesh processing tool. In: Eurographics Italian Chapter Conference. 2008;129-136.
17. Hoffmann J, Henning A, Giapitzakis IA, Scheffler K, Shajan G, Pohmann R, Avdievich NI. Safety testing and operational procedures for self-developed radiofrequency coils. *NMR Biomed* 2016;29(9):1131-1144.
18. Yarnykh VL Actual flip-angle imaging in the pulsed steady state: a method for rapid three-dimensional mapping of the transmitted radiofrequency field. *Magn Reson Med* 2007;57(1):192-200.
19. Wiggins GC, Triantafyllou C, Potthast A, Reykowski A, Nittka M, Wald LL. 32-channel 3 Tesla receive-only phased-array head coil with soccer-ball element geometry. *Magn Reson Med* 2006;56(1):216-223.
20. Giantsoudi D, De Man B, Verburg J, Trofimov A, Jin Y, Wang G, Gjestebj L, Paganetti H. Metal artifacts in computed tomography for radiation therapy planning: dosimetric effects and impact of metal artifact reduction. *Physics in Medicine and Biology* 2017;62(8):R49.
21. Gjestebj L, De Man B, Jin Y, Paganetti H, Verburg J, Giantsoudi D, Wang G. Metal artifact reduction in CT: where are we after four decades? *IEEE Access* 2016;e45826-5849.

22. Joemai R, de Bruin PW, Veldkamp WJ, Geleijns J. Metal artifact reduction for CT: Development, implementation, and clinical comparison of a generic and a scanner-specific technique. *Medical physics* 2012;39(2):1125-1132.

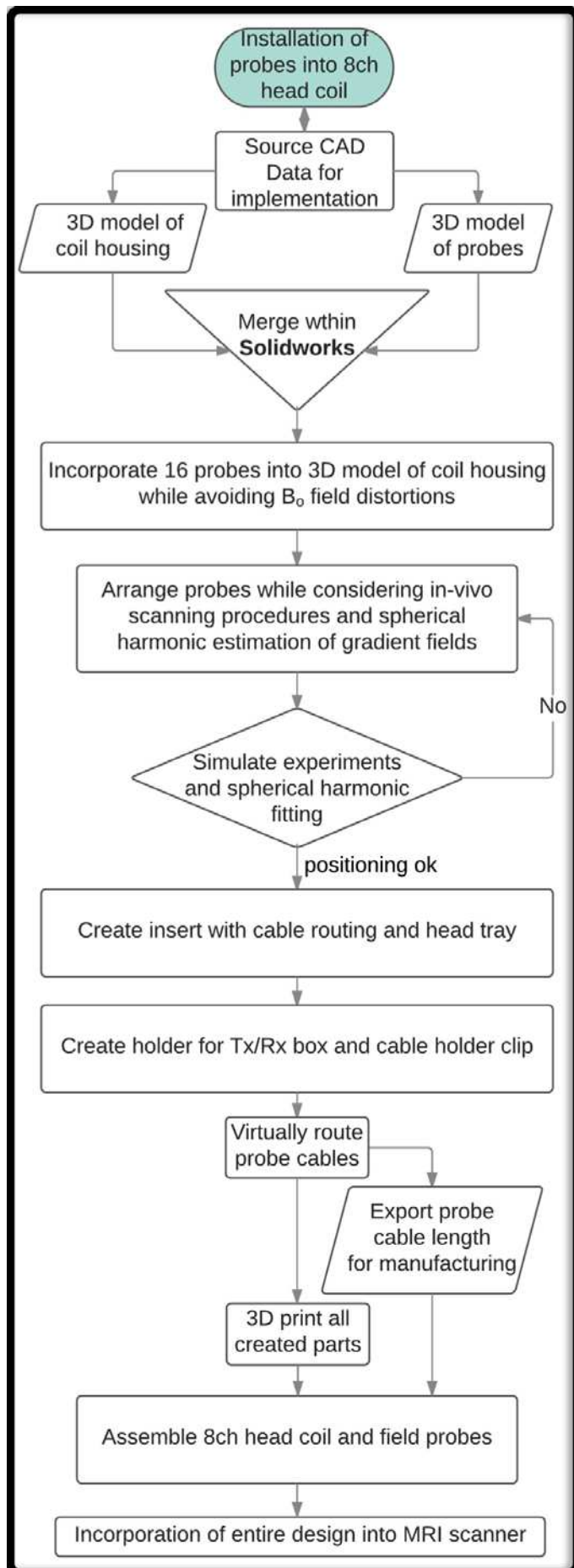


Figure 1. Flow chart for installing the probes and the corresponding Tx/Rx box into the 8ch coil. Bold-faced letters indicate a software package. CAD = computer aided design and compatible file types.

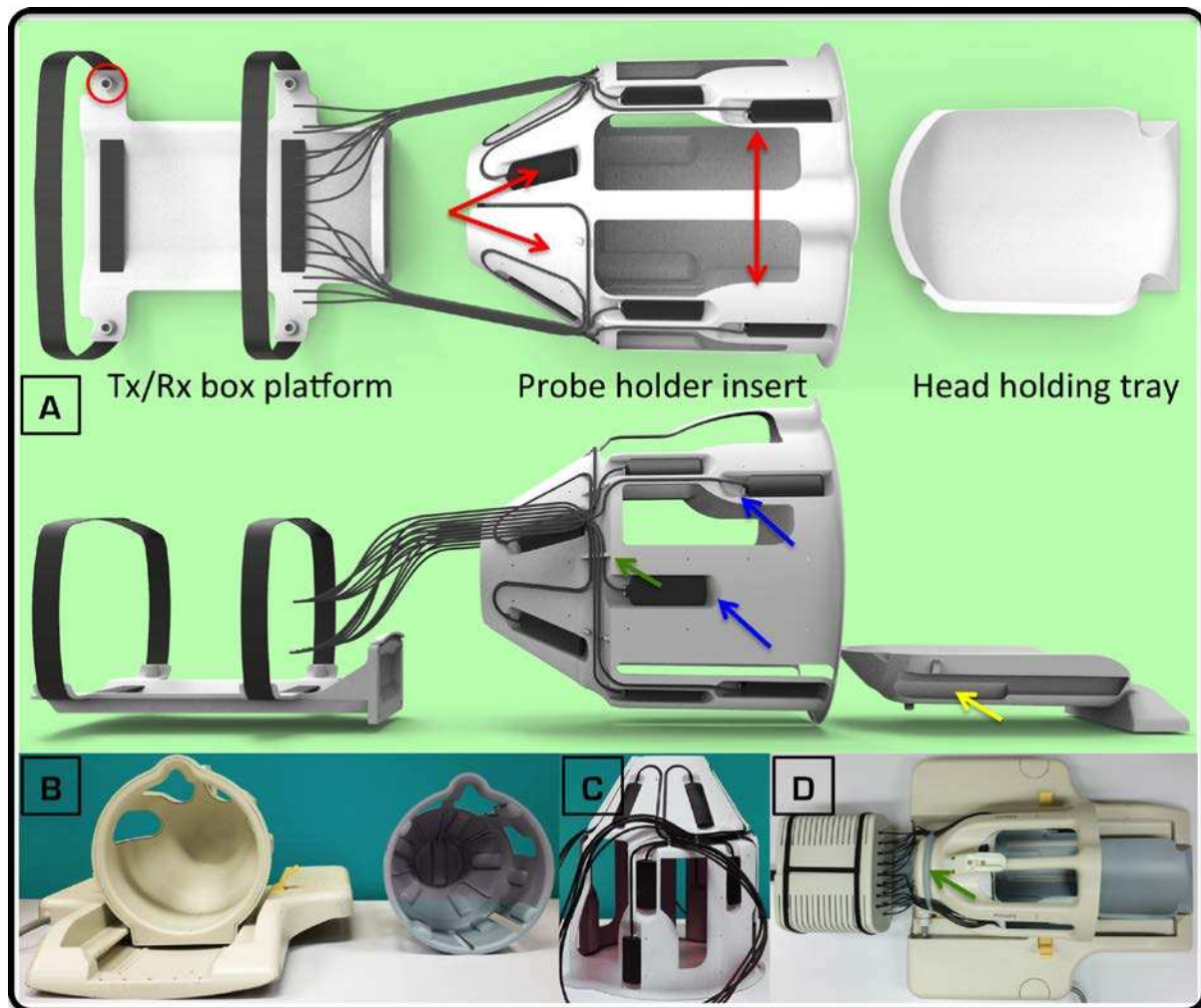


Figure 2. Several criteria of the design process are illustrated. (A) computer-generated renderings of the 3D model for three of the parts. (B-D) Photographs of different stages of assembly. In (B) the original 8ch coil is shown on the left and the probe holder insert on the right. The probes are installed into the insert in (C). Note the organized guiding of all the cabling. The red arrows highlight the left-right symmetry of the probe holder insert despite the asymmetric arrangement of the probes in that dimension. The blue arrows point to the gentle sloping of the probe holder insert in the direction of the 3T main magnetic field near the probes. A red circle indicates one of the pegs of the platform for the Tx/Rx box, which helps withstand the weight of the additional cabling toward the faraday cage during movement of the scanner table. The yellow arrow highlights grooves in the head holder tray that accommodate probes that had to be installed underneath. Note the larger clip at the back of the 8ch head coil and the smaller ones on the insert near the probes (green arrows). These clips secure and guide the cabling between the probes and the Tx/Rx box. The actual magnetic field probes are housed within the black rectangular objects. The green arrow in (D) points to the 4th 3D printed component of the design that is not depicted in (A).

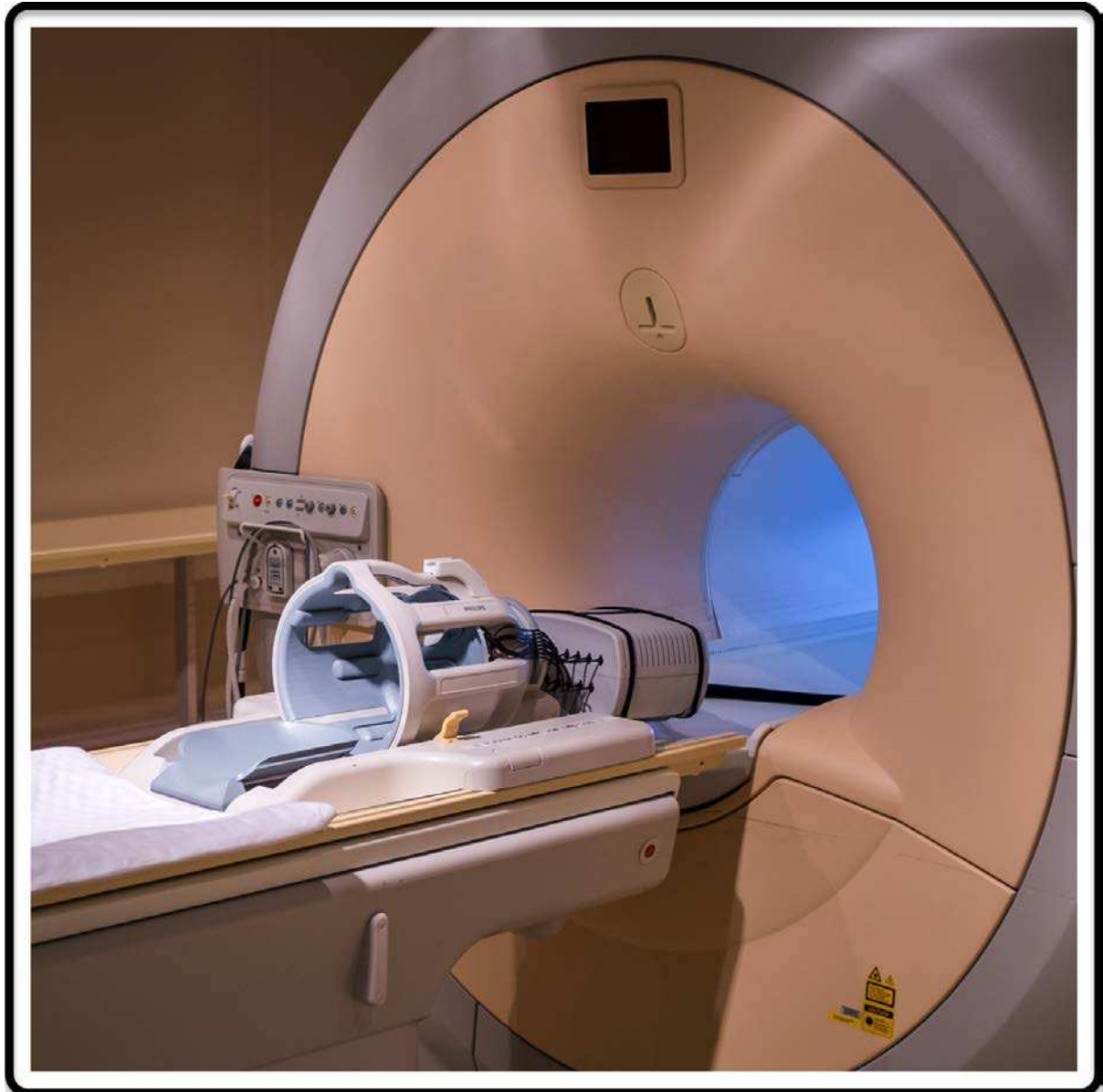


Figure 3. Final installation into the 3T MRI scanner.

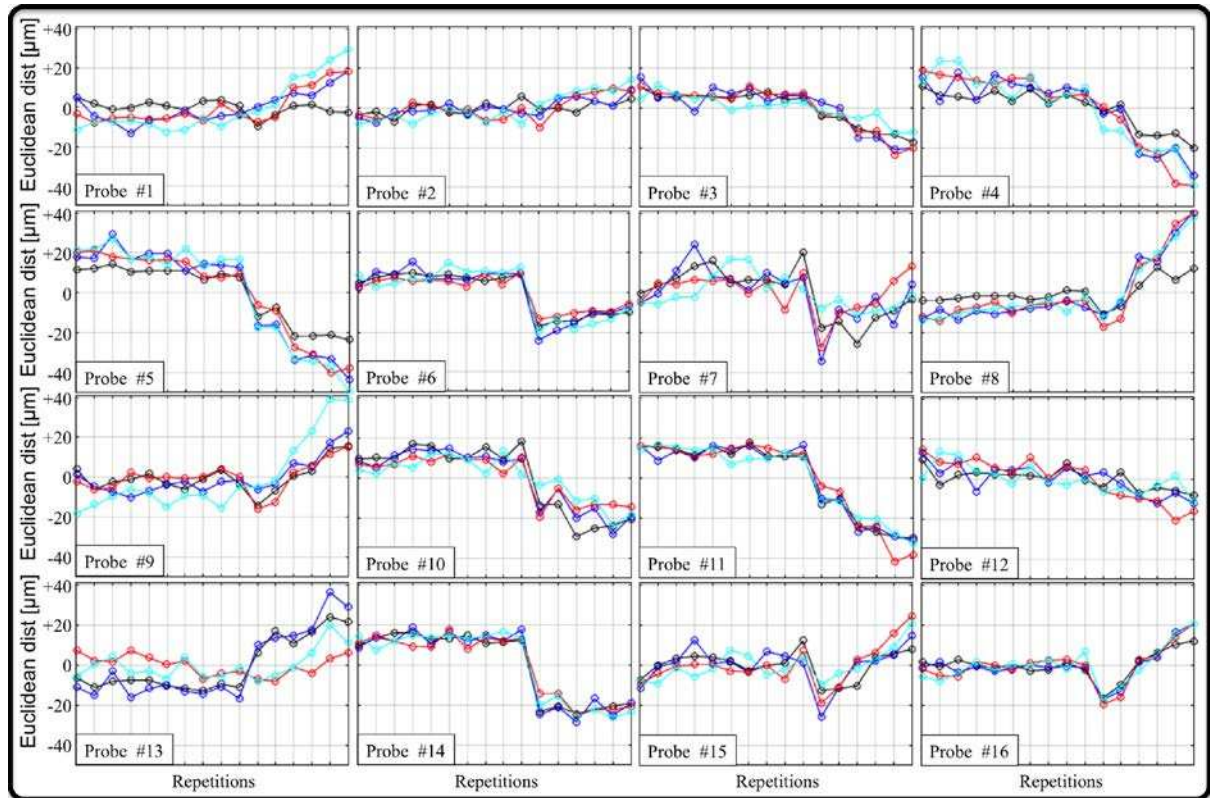


Figure 4. Reproducibility of positions of the 16 probes during an MRI experiment. The positions of the 16 probes were measured with a calibration experiment 16 times, with interleaved diffusion-weighted images after 10, 12, 14 calibrations. The x-axis of each plot indicates the 16 measurements while the y-axis provides the Euclidean distance from the isocentre. The different colors represent four different measurements on different days over four weeks.

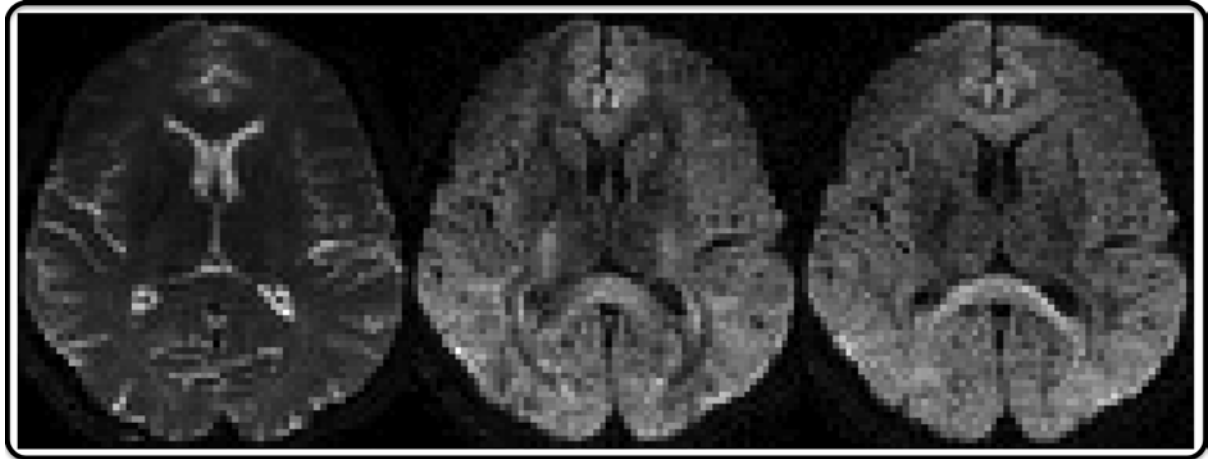


Figure 5. Representative images from a diffusion-weighted imaging data set. The leftmost image is the reference image without diffusion weighting while the other two images were collected with different diffusion encoding directions ($b = 1000 \text{ s/mm}^2$).

Supporting material

There are crucial differences between a CAD model and other 3D models. While CADs are parametric files that can be freely manipulated and scaled to precise dimensions other 3D models formats do not necessarily correspond to real-world coordinates. In our case the CAD model was created manually, while using the CT scan slices only as reference. Hence its correspondence to the actual physical coil was not perfect. There were two ways to ascertain that the CAD model corresponded to the physical 8ch coil. One of these would have required iterative 3D printing of the CAD design, assembly of the set up, noting the imperfections and refinement of the CAD model. The other method, which we chose to use, was the reconstruction of a 3D (not CAD) model of the coil housing from the CT scans. This 3D model was also not perfect because metal artifacts in CT scans create errors in the surface of the model. However, the overall shape of the model scaled with reliable internal dimensions. Alignment and scaling of the manually created CAD model against the rugged 3D model resulted in a convenient and perfectly parametric CAD model that was in near perfect correspondence with the real 8ch coil.

To create the 3D (not CAD) model required the following steps. The initial surface reconstruction was made in 3D Slicer. Utilizing the editor and model maker module an image intensity threshold was set to best match the plastic covering of the coil. The resulting 3D model of the coil housing was exported as a tessellated surface in .STL format. The reconstruction suffered from common errors such as duplicated or unreferenced vertices, non-manifold edges, duplicated faces etc. Correction required manual editing in Meshlab with the built-in cleaning and repairing filters. Subsequently, re-meshing filters were used to reduce the polygon count from approximately 20 million to near 2 million. This reduction did not hinder subsequent steps but significantly reduced computational overhead. Reconstruction of the outer surface of the plastic covering was further hindered by streaking metal artifacts that are commonly seen in CT. These artifacts pierce holes through the virtual surface of the plastic covering, which also required manual editing within Meshmixer.

Once again, following such a dual pathway proved necessary because Meshlab and Meshmixer produce tessellated meshes. These meshes are not parametric and not fully compatible with traditional CAD software, such as Solidworks. Nevertheless, these separate tessellated meshes served as an

independent reference for the actual parametric CAD model that was created in Solidworks.

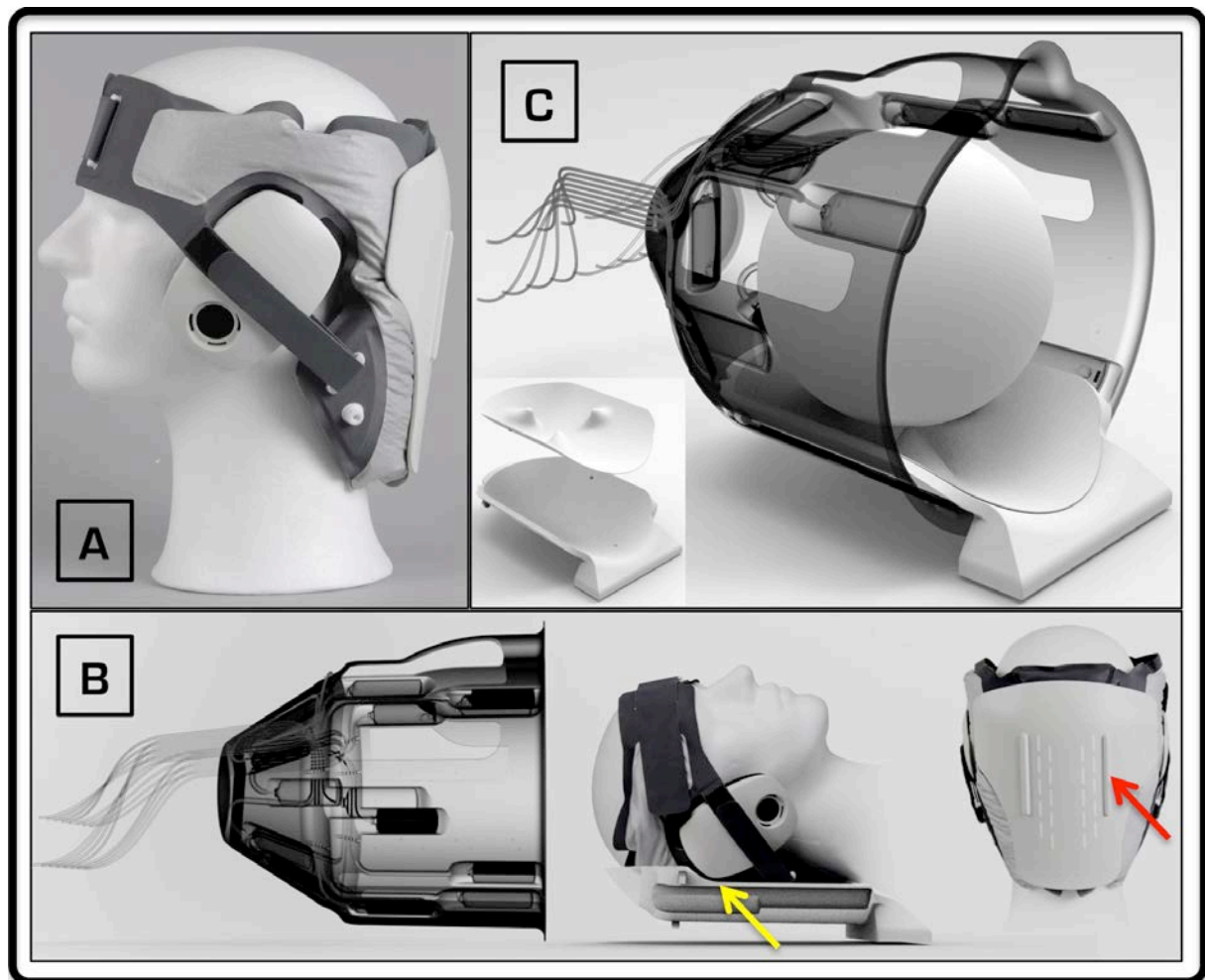
Please note, that we used both Meshmixer and Meshlab in creating the 3D model of the coil housing. Although in principle these two software packages possess partially overlapping set of tools, Meshmixer struggled with the initial output from 3D Slicer that had 20 million vertices. Once the model was cleaned up and the number of vertices reduced 10-fold, the additional tools for manual editing could be utilized in Meshmixer.

Type	Design criteria or boundary condition	Short description and reasoning
Ergonomics / comfort	Secure cabling outside head coil	To ensure safe and robust usage the cables were secured with a 3D printed clip to the back of the coil.
	Secure and ergonomic cabling inside head coils	To aid installation and dismounting the insert had unique clips for each of the probes and its cable. This avoided tangled cables and helped minimize cable length.
	Comfort of volunteer	The final design must be comfortable and aesthetically acceptable both to meet ethical guidelines and to avoid a confound or noise source in cognitive neuroimaging experiments from undue apprehension of the volunteer.
	Easy maintenance of hygiene	The 3D printing material was chosen so that it could be either easily cleaned or coated to be wipeable.
MRI experimental procedures	Compatibility of Tx/Rx box with fMRI experiments	Often fMRI experiments use a projection screen behind the scanner. The Tx/Rx box, which optimally should be near the probes, was placed at the lowest possible position along the vertical laboratory coordinate.
	Maintaining unobstructed view from head coil for claustrophobic volunteers and/or fMRI experiments	Finding the optimal position for probes was an iterative process, ensuring no probe would be in front of either eye or above the nose while ensuring that the constellation still allowed for the spherical harmonic fitting. Furthermore, although the position of the probes was asymmetric the 3D printed insert was symmetric to ensure identical obstruction of both left and right field of view.
	Compatibility of Tx/Rx box with fMRI experiments	Often fMRI experiments use a projection screen behind the scanner. The Tx/Rx box, which optimally should be near the probes, was placed at the lowest possible position along the vertical laboratory coordinate.
Safety	Avoiding contact to probes during experiments	Although plastic covering protects the probes, it was considered important to avoid contact of the plastic covering and the skin of the volunteer.
	Compatibility with emergency procedures	Because in a case of emergency the volunteer must be rapidly removed from the scanner room it was imperative that the sliding function of the 8ch head coil remained intact.
	Avoiding cables along volunteers' body	The Tx/Rx box position and the routing of cables were made toward the back of the scanner after leaving the head coil.

Technical	Constant & minimum cable length	To ensure ergonomic and safe operation cable length between probes and Tx/Rx box was minimized. A platform for the Tx/Rx box was secured to the base of the 8ch head coil using the already available screws.
	The solution for securing the probes to the head coil should take up minimal space.	For optimal SNR, head coils are typically small in diameter. The 3D printed insert is 800 μm in thickness.
	Optimal positioning of probes within 8ch head coil	The 8ch coil slides back and forth to aid positioning the volunteer, which necessitates a head holding tray. The original tray does not have clearance to fit probes underneath it within the head coil. The redesigned tray was 3D printed with grooves to accommodate the probes without putting pressure on them.
	Robust installation of Tx/Rx box around head coil	The Tx/Rx box is connected to the faraday cage with a long bundle of the 16 cables. To avoid the weight of this cable bundle pulling the Tx/Rx box out of position the 3D printed platform was designed with pegs matching the position of the feet of the Tx/Rx box.
	Avoiding disturbance of B_0 field of scanner	Both the 3D printing material and the shape of this material were considered to avoid local distortions of the main magnetic field in the vicinity of the probes.
	Semi-permanent installation	It was important that the installation was stable and long-lasting but also disassembly would be easy in case of repair or if the probes were installed into another head coil.
	Installation must not void warranty of MRI head coil	It was of course of paramount importance that the installation remained within the boundaries of the service contract of our scanner.
	Stabilization of probes during experiments	For optimal operation the probes should be immobile during experiments. A regular grid of holes were scattered in the insert where with small drops of glue the insert could be stabilized against subject movement.

	3D printing guidelines	3D printing technology has its own boundary conditions, such as minimum thickness of material, minimum size of holes, incompatibility with completely closed volumes etc.
Miscellaneous	Reproducibility and cost effectiveness	Manufacturing must not only be reproducible for easy iterations of current design but also flexible enough for future versions (e.g. different head coils). Further, the different parts should be manufactured with the fewest number of techniques to reduce dependency on differing delivery times of suppliers.
	Easily distributable product or method	We also maintained the view that the final product should be easy to share with other laboratories.

Supporting Table S1. List of boundary conditions and design criteria.



Supporting Figure S1. Two examples where a 3D model of the coil housing is useful. (A & B) Prototype from an ongoing project on a head stabilization system. For example this system may incorporate extruded parts (red arrow) that easily lock into corresponding grooves in the head holder tray (not shown) to limit rotations around the anterior/posterior axis. The design of head stabilization system is further aided by the 3D model of the head coil housing and head holder tray to ensure the hearing protection headphones are compatible with the head holding tray (yellow arrow) or the arrangement of the probes inside the coil. (C) Prototype of a bespoke phantom holder that fits perfectly inside the head holder tray to help position a spherical phantom accurately and precisely to the center of the coil. This aids both experiments and quality assurance measures because it reduces unwanted variance that arises from inconsistent positioning and helps simplify post processing code that need not detect the position of the phantom within an image.

Supporting Video S1. Animated illustration of the key steps of the design pipeline for installing the probes, cabling and Tx/Rx electronics around an 8ch MRI head coil.